Preprint Title	Innovative and scalable PHMB-containing nanoemulsion based on a blend of rosehip and sunflower oils for wound healing applications
Authors	Mariana F. Alves-Silva, Eron L. Alves-Pereira, Daniele C. Gomes, Ednaldo G. do Nascimento and Arnóbio A. Silva-Júnior
Publication Date	05 Aug. 2026
Article Type	Full Research Paper
ORCID® iDs	Mariana F. Alves-Silva - https://orcid.org/0000-0001-9373-3585; Eron L. Alves-Pereira - https://orcid.org/0009-0006-8305-948X

Innovative and scalable PHMB-containing nanoemulsion based on a blend of rosehip and sunflower oils for wound healing applications

Mariana Farias Alves da Silva*[1,2‡], Eron Lincoln Alves-Pereira[2‡], Daniele Cavalcante Gomes[1], Ednaldo Gomes do Nascimento[2], and Arnóbio Antônio da Silva-Júnior[2]

[1]Research and Development Department, ISnano – Innovation and Solutions in Nanotechnology Ltd., Av. Alberto Santos Dumont, 1560, Macaíba, RN, Brazil, 59.288-899.

[2]Pharmacy Department, Federal University of Rio Grande do Norte, Gen. Gustavo Cordeiro de Faria Street, Petrópolis, Natal, Rio Grande do Norte, Brazil, 59012-570.

Mariana Farias A. da Silva – marianafarias0011@gmail.com / mariana.farias@isnano.com.br

* Corresponding author

‡ Equal contributions

Abstract

Multifunctional nanobiomaterials that combine antimicrobial activity with enhanced tissue repair is highly desirable in wound care. In this study, a low energy nanoemulsion based on rosehip and sunflower oils containing polyhexamethylene biguanide (PHMB) was developed and characterized as a potential nano-ingredient for topical application. The formulation exhibited nanometric droplet size, low polydispersity, and good physicochemical stability, maintaining its properties under different storage conditions and across scalable production batches. Biological evaluation demonstrated antioxidant activity associated with the vegetable oils, as well as enhanced antimicrobial efficacy compared to PHMB solution. In addition, the formulation reduced the expression of pro-inflammatory cytokines (IL-1, IL-6, and TNF-α) and promoted accelerated human epidermal keratinocytes migration in the wound healing assay *in vitro*, indicating combined anti-inflammatory and regenerative effects. Overall, the results suggest that this platform represents a promising multifunctional system for wound management, integrating antimicrobial protection with improved tissue repair.

Keywords

vegetable oils; antioxidant; anti-inflammatory; nanoingredient; polyhexamethylene biguanide.

Introduction

Skin lesions represent a significant clinical and public health concern, since effective wound healing is essential to restore tissue integrity and prevent infections. The wound healing process is a complex and dynamic sequence of events involving inflammation, proliferation, and tissue remodelling, which must occur in a coordinated manner to achieve successful repair. Interruption of any of these steps can lead to delayed healing and increased susceptibility to microbial colonization, highlighting the need for therapeutic strategies capable of simultaneously promoting tissue regeneration and controlling microbial growth [1,2].

Natural oils have been receiving increasing attention in dermatological and cosmetic formulations due to their bioactive composition and beneficial effects on skin repair [3]. Among them, sunflower oil (*Helianthus annuus*) is rich in essential fatty acids, particularly linoleic acid, which contributes to the maintenance of skin barrier function and supports epidermal repair [4]. Another natural compound that is widely recognized for its moisturizing, antioxidant, and regenerative properties is rosehip oil (*Rosa canina* or *Rosa rubiginosa*). Rosehip oil contains high levels of polyunsaturated fatty acids, carotenoids, and phenolic compounds, which are associated with antioxidant activity and skin regeneration stimulation [5]. Despite these beneficial properties, the therapeutic effectiveness of these oils may be limited by factors such as poor stability, low bioavailability, and limited penetration into the skin [6].

Nanostructured delivery systems, particularly nanoemulsions, have emerged as promising platforms for enhancing the bioactive performance in topical formulations [7]. Nanoemulsions (NE) are characterized by droplet sizes typically

ranging from 20 to 200 nm, which provide advantages such as improved stability, increased surface area, enhanced skin penetration, and controlled release of active ingredients. These properties make nanoemulsions attractive systems for the delivery of natural oils and other bioactive molecules intended for wound care applications [8].

Beyond the scope of tissue regeneration, preventing microbial contamination stands as a critical determinant of successful wound healing [9,10]. Polyhexamethylene biguanide (PHMB) is a broad-spectrum antimicrobial agent widely used in medical and wound care products due to its high efficacy against bacteria and relatively low cytotoxicity to mammalian cells [11]. PHMB acts primarily by disrupting microbial cell membranes, leading to rapid antimicrobial activity. Beyond its antimicrobial properties, recent studies suggest that PHMB may also contribute indirectly to wound healing by reducing microbial burden and maintaining a favourable environment for tissue regeneration [12].

The combination of bioactive oils with antimicrobial agents in nanostructured systems may represent a promising strategy to develop multifunctional formulations capable of promoting skin repair while simultaneously preventing infection. In this context, the association of PHMB with a nanoemulsion formulated from a blend of sunflower and rosehip oils may enhance both the antimicrobial efficacy and the regenerative potential of the system.

Therefore, the present study aimed to develop and evaluate a nanoemulsion based on a blend of sunflower and rosehip oils associated with PHMB and to investigate its physicochemical properties and biological activities, including antioxidant, moisturizing, anti-inflammatory, antimicrobial, and wound healing effects.

Results

Characterization

The blank nanoemulsion (NE PHMB-Free) and the PHMB-loaded nanoemulsion (ISnanoBio® PHMB) exhibited identical droplet size distributions, with mean diameters ranging between 170 - 180 nm. In contrast, a significant distinct profile was observed for Zeta Potential (ZP). The NE PHMB-Free presented a negative surface charge of -19.2 ± 0.8 mV, whereas the incorporation of the cationic polymer in the ISnanoBio® PHMB shifted the net charge to near-neutrality (0.2 ± 0.1 mV) (**Fig. 1a–b**). Based on these promising initial findings, the ISnanoBio® PHMB formulation was selected for a scale-up process aiming at potential industrial applications.

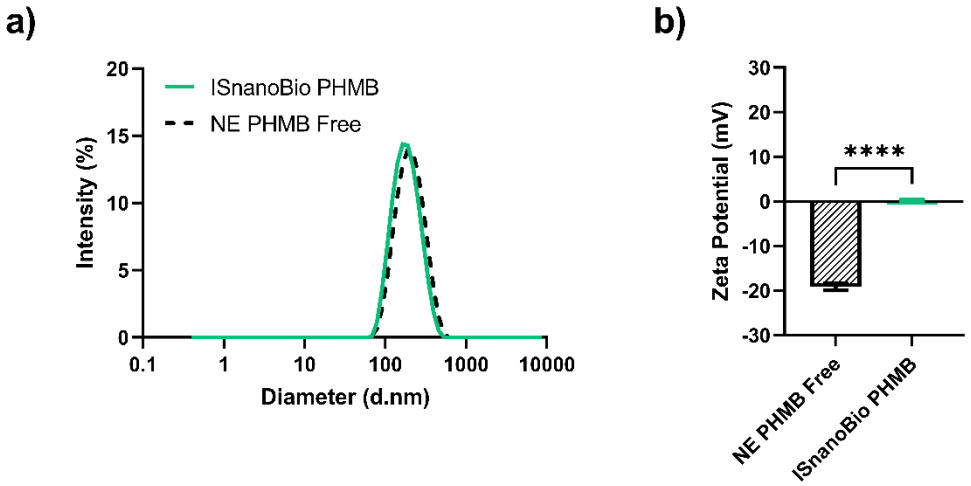

Figure 1: Physicochemical characterization of different nanoemulsions a) hydrodynamic diameter distribution; b) Zeta Potential (**** $p < 0{,}0001$).

Scaling

The formulation was successfully scaled up from 10 g laboratory samples to 30 kg pilot-scale batches (**Fig. 2**).

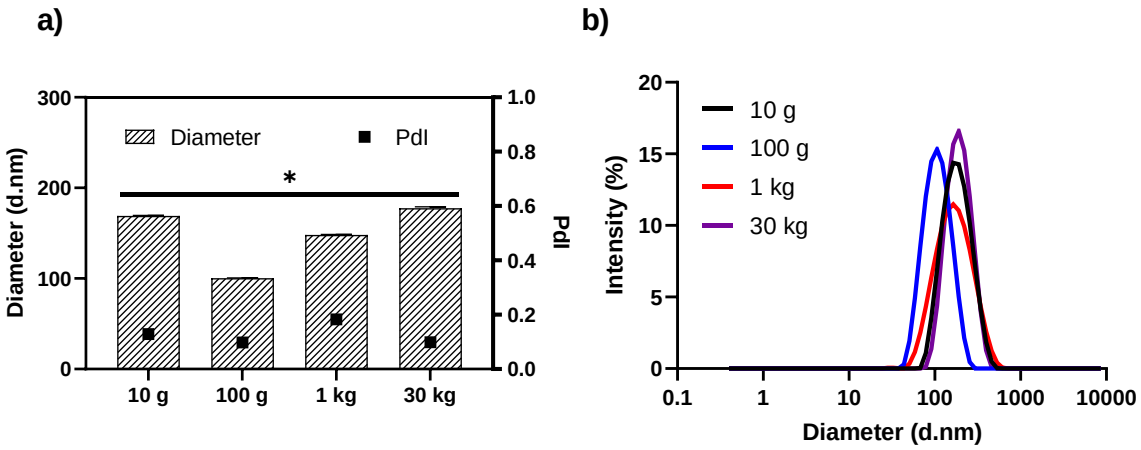

Figure 2: Physicochemical characterization of scaling test of nanoemulsions a) Diameter and PdI; b) Size distribution.

Although minor statistically significant differences in droplet size were observed among these batches, the mean diameters and polydispersity indices (PdI) consistently remained within the ideal range for nanotechnological systems. These findings confirm a narrow, monodisperse distribution for ISnanoBio® PHMB, demonstrating high process reproducibility even at a larger production volume.

Stability study

Throughout the entire monitoring period across all tested storage conditions, the ISnanoBio® PHMB formulations maintained their original macroscopic characteristics, showing no detectable alterations in appearance, color, or odor, and confirming the absence of phase separation or precipitation.

Apparent stability under Storage

Droplet size (**Fig. 3a**), zeta potential and pH (**Fig. 3b**) of ISnanoBio® PHMB stored under room temperature (25 ± 2 °C) were monitored for 180-day interval of time. Its nanometric scale remained throughout the entire y monitoring period (D1–D180). The mean droplet diameter started near 150 nm (D1–D7), experienced a transient increase to approximately 220 nm at D30, and subsequently decreased, stabilizing between 145 and 160 nm up to D180. Concurrently, PdI values remained low and stable, fluctuating between 0.15 and 0.25, which confirms a moderately narrow size distribution. The zeta potential displayed minor variations over time; initially near-neutral at D1–D7, ZP values shifted to around 3.0–3.5 mV at D30 and D60, before returning to approximately 1.0–2.0 mV by D90 and D180. Despite these fluctuations, no signs of phase separation or abrupt instability occurred. Furthermore, the pH remained essentially constant during storage, varying only slightly within the 4.3–4.6 range.

Accelerated and Stress Stability Tests

Under refrigerated storage (4 ± 2 °C) over a 15-day period (**Fig. 3c–d**), the ISnanoBio® PHMB also exhibited high physical stability. The droplet diameter hovered around 145–165 nm from D1 to D15, showing only a minimal increase at the final time point. The PdI values remained consistently low (0.13–0.18), indicating the preservation of a homogeneous droplet population. The ZP remained close to neutrality throughout the evaluation, rising slightly from 0.2 mV (D1) to 0.8 mV (D15), while the pH values were stable at approximately 4.4.

At an elevated temperature (45 ± 2 °C) (**Fig. 3e–f**), the formulation likewise sustained its nanometric characteristics. The droplet diameter remained virtually

unchanged (145–150 nm) from D1 to D15, and the PdI values stayed stable and low (0.12–0.16). The zeta potential exhibited a minor upward trend, rising from 0.3 mV at D1 to 0.9 mV at D15, with the pH showing minimal variation around 4.4.

Finally, during the thermal shock cycling test (4 ± 2 °C to 45 ± 2 °C) (**Fig. 3g–h**), the nanoemulsion demonstrated strong resistance to thermal stress. The droplet diameter was highly stable at approximately 145 nm throughout the entire challenge, with PdI values tightly controlled between 0.12 and 0.18. The zeta potential increased slightly over time (from 0.3 to 0.8 mV), while the pH remained constant at approximately 4.4.

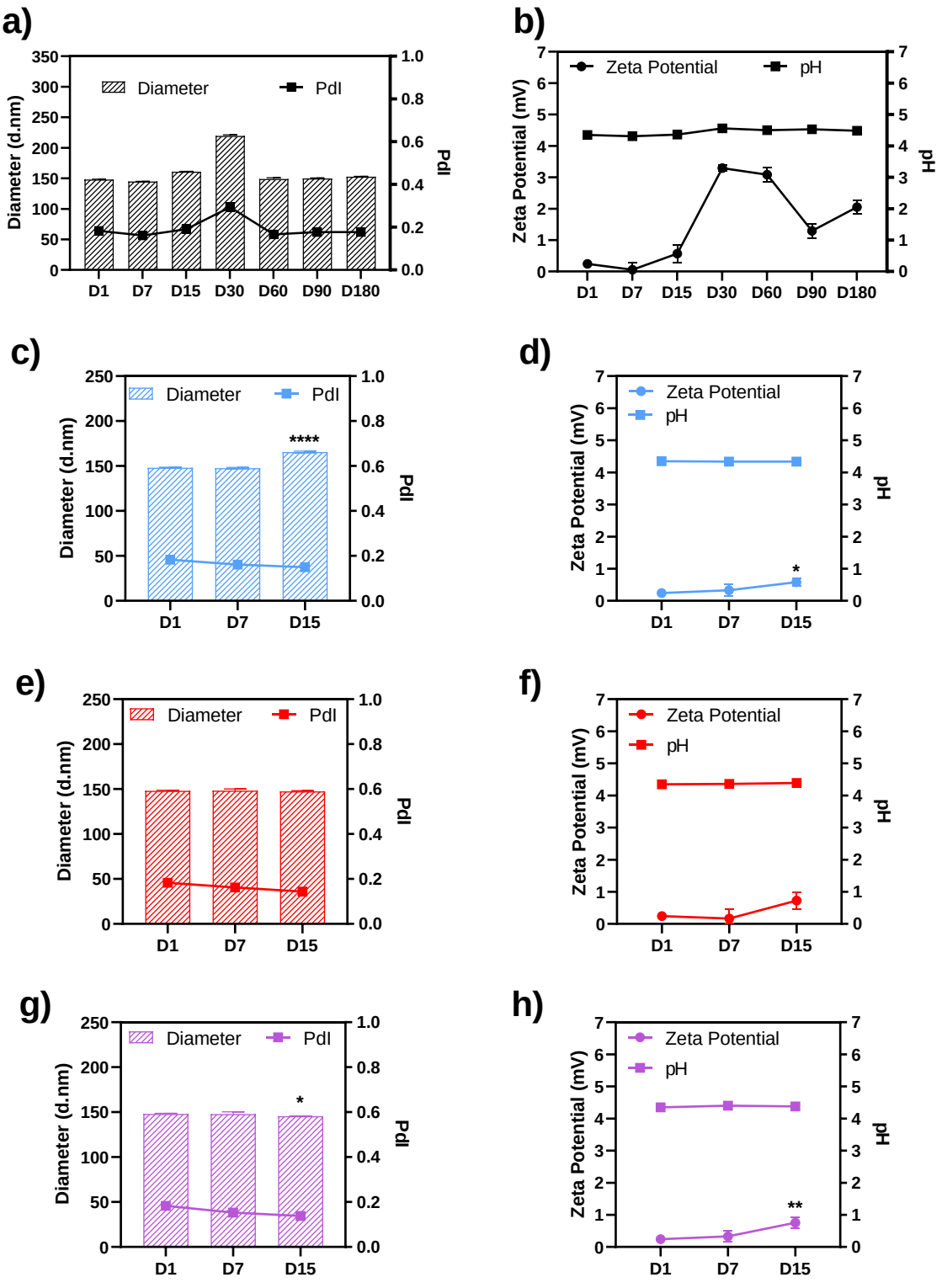

Figure 3: Diameter, PdI, Zeta potential and pH on stability evaluation of ISnanoBio® PHMB a) and b) 25 ± 2 °C; c) and d) 4 ± 2 °C; e) and f) 45 ± 2 °C; g) and h) 4 ± 2 °C – 45 ± 2 °C cycle.

Efficacy studies

Antioxidant activity

The DPPH scavenging assay (**Fig. 4a**) demonstrated the superior antioxidant activity of ISnanoBio® PHMB compared with a PHMB solution and a commercial PHMB-based product, evaluated under the same experimental conditions and equivalent PHMB concentrations. ISnanoBio® PHMB exhibited a DPPH radical scavenging capacity of 61.9%, whereas the commercial product showed 11.5%, and PHMB solution did not exhibit detectable antioxidant activity.

Moisturizing effect

The moisturizing effect was evaluated using an assay designed to assess the barrier function of the formulations. As shown in **Fig. 4b**, ISnanoBio® PHMB exhibited a moisturizing effect through this mechanism, showing reductions in transmembrane water loss of 25.1 ± 2.7% and 29.1 ± 1.6%, respectively.

Anti-inflammatory activity

The anti-inflammatory effects of ISnanoBio® PHMB, PHMB solution, and a commercial PHMB Solution were evaluated by assessing the modulation of pro-inflammatory cytokine expression, including Interleukin-1 (IL-1), Interleukin-6 (IL-6), and Tumor Necrosis Factor-α (TNF-α). The IL-1 modulation profile (**Fig. 4c**) showed a downregulation of cytokine expression promoted by ISnanoBio®, inhibiting 20.3 ± 3.9% of IL-1 expression. PHMB solution, and the commercial PHMB Solution showed inhibition values of 5.9 ± 6.5%, and 8.3 ± 7.8%, respectively, which were not considered statistically significant.

IL-6 expression (**Fig. 4d**) exhibited the most pronounced reduction among the evaluated cytokines. ISnanoBio® PHMB reduced IL-6 expression by 60.1 ± 2.9%, PHMB solution by 78.3 ± 1.7%, and the commercial PHMB Solution by 58.3 ± 2.6%. For TNF-α expression (**Fig. 4e**), the samples showed inhibition values of 22.4 ± 2.3%, 32.8 ± 1.2%, and 18.8 ± 5.5% for ISnanoBio® PHMB, PHMB solution, and the commercial PHMB solution, respectively.

In Vitro Wound Healing

The wound healing assay evaluated the capacity of the formulations to accelerate scratch closure in human keratinocyte monolayers over a 48 h period. Quantitative kinetic measurements were performed at 12, 24, 36, and 48 h (**Fig. 4f**), and representative micrographs capturing the initial, intermediate, and final stages of scratch closure are presented in **Figure 5**. At the baseline (0 h), all experimental and control groups exhibited equivalent wound areas, establishing a uniform starting point for analysis.

Initial scratch closure rates after 12 h were similar across all tested groups, with ISnanoBio® PHMB reaching 14.3 ± 1.3%, followed by the free PHMB solution (12.6 ± 2.1%), the commercial PHMB-based product (12.4 ± 0.8%), and the untreated control (11.8 ± 1.2%). However, a dramatic divergence was observed at the 24 h mark; the ISnanoBio® PHMB group promoted a substantial increase in cell migration, achieving 74.2 ± 2.3% wound closure, markedly outperforming the commercial product (64.2 ± 5.6%), the control group (65.2 ± 2.1%), and the free PHMB solution (58.6 ± 3.1%). This superior performance was sustained at 36 h, with the nanoemulsion leading to 86.9 ± 2.2% closure, compared to 80.6 ± 1.9% for the control.

Finally, at 48 h, complete wound closure (100%) was successfully achieved in both the ISnanoBio® PHMB and the commercial product groups, whereas the free PHMB solution and the control group lagged behind, plateauing at approximately 90.4 ± 0.5% and 90.7 ± 3.4% closure, respectively.

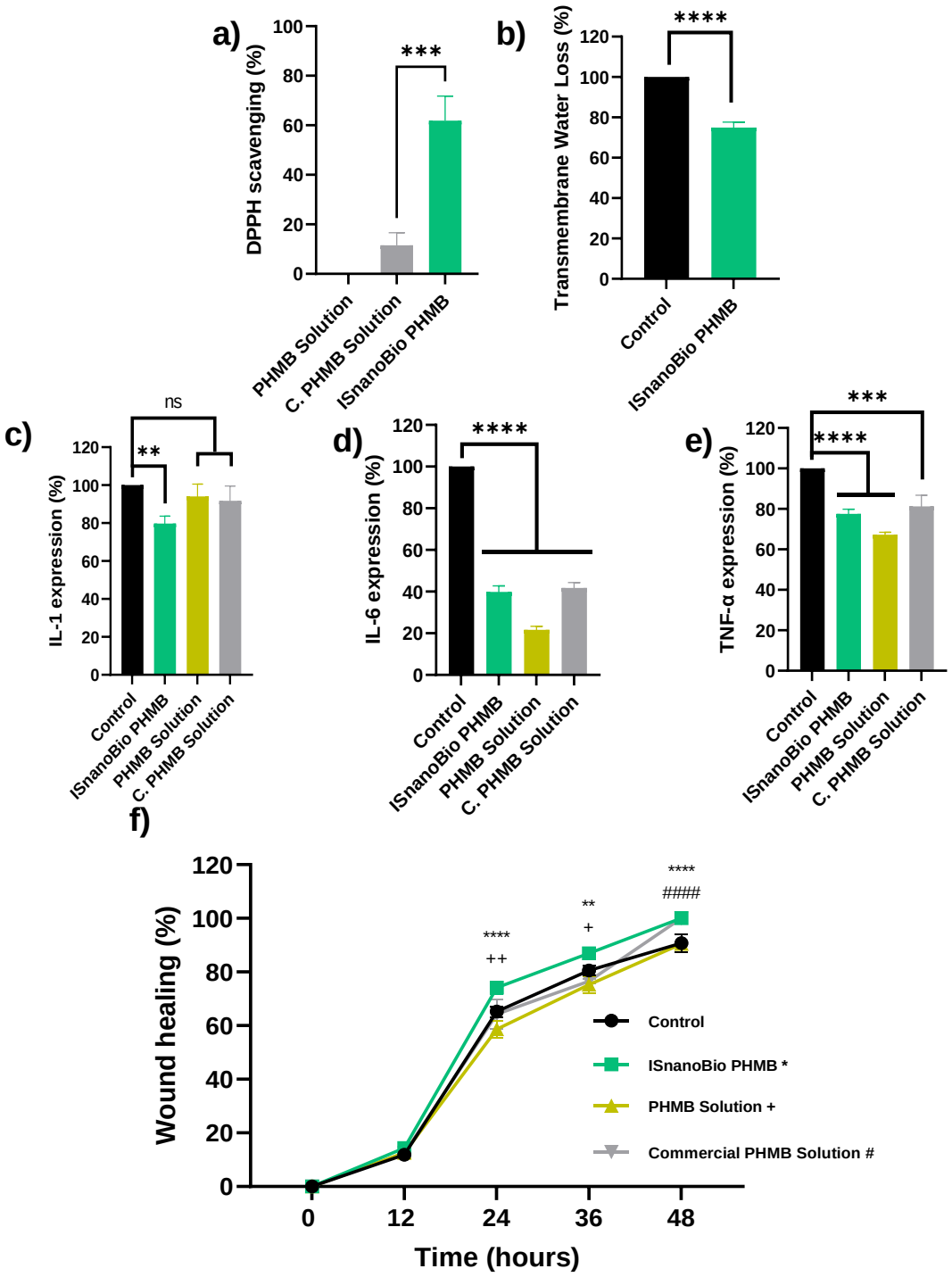

Figure 4: *In vitro* efficacy studies a) DPPH scavenging; b) Transmembrane water loss; c) IL-1 expression; d) IL-6 expression; e) TNFα expression; f) Percentage of wound closure (* IsnanoBio PHMB, + PHMB Solution, # Commercial PHMB Solution.)

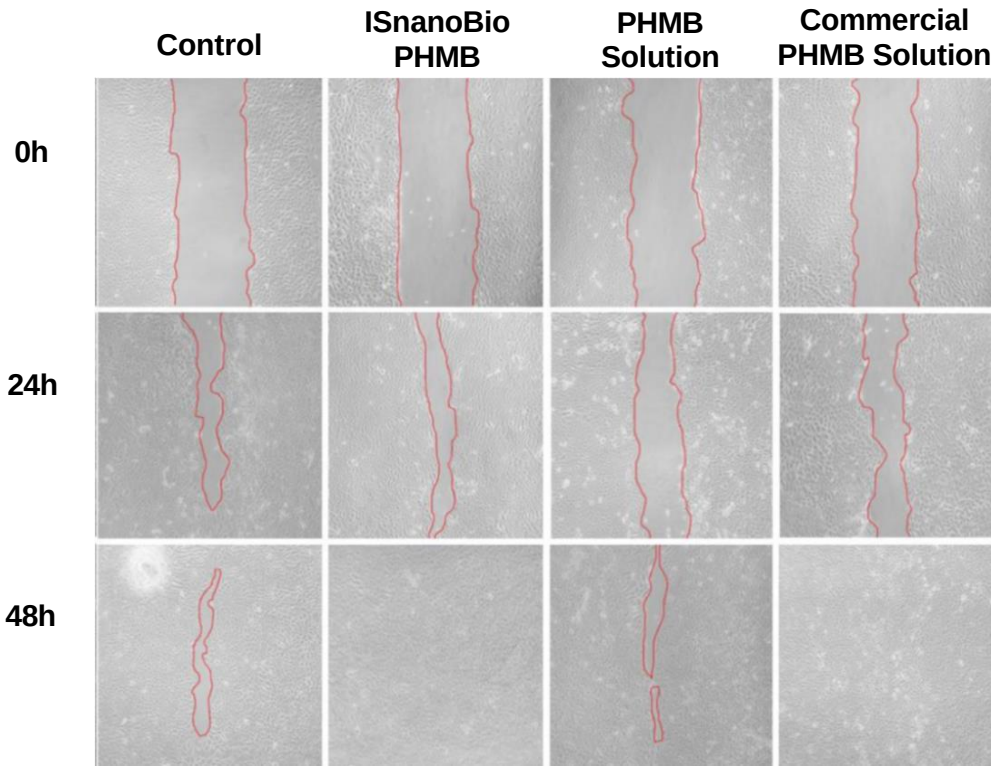

Figure 5: *In vitro* wound closure at 0, 24 and 48 hours after treatment

Antimicrobial effect

To assess the antimicrobial activity of ISnanoBio® PHMB, a Minimum Inhibitory Concentration (MIC) assay was performed, comparing the formulation with PHMB solution, a Commercial PHMB Solution, and the free oils blend (rosehip and sunflower). The results are presented in **Table 1** and demonstrate the enhanced activity promoted by the combination of PHMB with nanostructured oils.

ISnanoBio® PHMB showed MIC values of 1:16 against *Staphylococcus aureus* and an impressive >1:64 against *Escherichia coli*, while PHMB solution showed MIC values of 1:4 and 1:16, respectively. The Commercial PHMB Solution

presented MIC values of 1:32 and 1:16, whereas the oils showed MIC values of 1:2 and >1:2.

Table 1: Minimum inhibitory concentration of samples.

Sample	**MIC (dillution)**	
	S. aureus	***E. coli***
ISnanoBio PHMB	1:16	<1:64
PHMB Solution	1:4	1:16
Commercial PHMB Solution	1:32	1:16
Free oils blend	1:2	>1:2

Discussion

This study aimed to develop, characterize, scale up, and evaluate a novel nanoemulsion based on a blend of sunflower and rosehip oils associated with PHMB as a potential wound healing system, elucidating the influence of this biguanide on the physicochemical and therapeutic characteristics of the nanoemulsion. The characterization showed that PHMB does not influence the droplet diameter; however, it significantly altered the surface charge profile. The blank nanoemulsion (NE PHMB-Free) exhibited anionic zeta potential, which shifted toward neutrality upon the addition of PHMB. This charge reversal is directly attributed to the chemical nature of PHMB, a highly cationic polymer containing protonated amine groups.

These positively charged moieties interact with the droplet interface, allowing the polymer to adsorb onto and coat the surface of the nanostructures. Similar interfacial behaviors and charge masking have been reported in studies involving polymeric nanoparticles [13] and polymeric aggregates [14].

Following the elucidation of the role of PHMB in the interfacial properties of the system, a scale-up study was performed to evaluate the feasibility of manufacturing the nanoemulsion at a pilot-industrial scale. The results demonstrated that the fundamental nanotechnological characteristics were successfully maintained across all batch sizes, with minor variations being attributed to the specific shear profiles applied during each preparation. The bench-scale batch (10 g) was produced via magnetic stirring, a process characterized by low, localized shear forces. In contrast, the larger batches utilized mechanical agitation; within these scaled-up systems, a slight trend toward increased droplet size was observed as the formulation volume escalated, culminating in the 30 kg batch. This behavior is well-documented in process engineering and is explained by the progressive challenge of achieving uniform shear dissipation and homogeneous energy distribution throughout larger fluid volumes [15].

Driven by the evidence that the formulation is highly scalable via the phase inversion method, its long-term stability was sequentially thoroughly investigated under diverse storage conditions. The nanosystem successfully maintained its droplet diameters within the nanometric range, preserved low polydispersity, and exhibited stable zeta potential and pH values over the monitoring periods. These findings underscore a highly satisfactory physicochemical stability, a particularly notable achievement given that the system was manufactured using a low-energy emulsification approach. This colloidal robustness can be primarily attributed to the

efficient steric stabilization provided by the surfactant combination of polysorbate 80 and poloxamer 407. The hydrophobic segments of these amphiphilic molecules anchor firmly at the oil interface, while their hydrophilic chains extend into the aqueous phase, generating a powerful steric hindrance that prevents close droplet–droplet interactions and effectively inhibits coalescence [16,17]. Additionally, the small droplet size and low polydispersity contribute to the stability, as they enhance Brownian motion and reduce destabilization phenomena such as Ostwald ripening [18,19].

Following the physicochemical characterization and stability trials, the bioactivity of the formulation was investigated. The DPPH radical scavenging assay demonstrated a remarkable antioxidant potential for the nanostructured system. While free PHMB itself does not exhibit inherent radical scavenging properties, the vegetable oils comprising the nanoemulsion core contribute significantly to this effect. Both sunflower and rosehip oils are naturally rich in bioactive components, including unsaturated fatty acids, phenolic compounds, carotenoids, and tocopherols. In particular, the high content of these lipophilic antioxidants in rosehip oil plays a pivotal role, as they readily donate hydrogen atoms or electrons to neutralize free radicals, thereby imparting substantial antioxidant activity to the final formulation [20,21].

The moisturizing effect experiment evaluated the occlusive capacity of the formulations and demonstrated this property for ISnanoBio® PHMB. This effect can be attributed to the lipophilic nature of the oils, which form a thin film on the surface of the membrane, thereby reducing transmembrane water loss and consequently transepidermal water loss [22]. The formation of this film is facilitated by the nanometric-sized droplets, which enhances oil spreading and increases the surface

area coverage, contributing to the observed occlusive and moisturizing effects. Several studies have demonstrated that effect [23–25].

The anti-inflammatory evaluation demonstrates the PHMB nanodevice potential in reduce inflammation through the modulation of pro-inflammatory cytokine expression. For IL-6 and TNF-α, all formulations promoted a decrease in their expression levels. However, for IL-1, only ISnanoBio® PHMB was able to significantly reduce IL-1 levels, highlighting the superior anti-inflammatory performance of this formulation.

The anti-inflammatory effect observed for the PHMB nanoemulsion may be attributed to the combined action of the bioactive compounds present in the vegetable oils and the antimicrobial activity of PHMB. Unsaturated fatty acids and antioxidant molecules such as tocopherols and carotenoids are known to modulate inflammatory signaling pathways, including NF-κB, leading to reduced expression of pro-inflammatory cytokines such as IL-1, IL-6, and TNF-α [26,27]. Additionally, the antimicrobial activity of PHMB may decrease inflammatory stimuli associated with microbial presence, further contributing to cytokine downregulation [28–30].

The *in vitro* wound healing assay demonstrated that the nanoformulation significantly accelerated keratinocyte migration compared to both the untreated control and the commercial comparator, with the most pronounced divergence occurring at the 24 h mark. Notably, ISnanoBio® PHMB achieved the highest wound closure rate, culminating in complete scratch sealing within 48 h.

This enhanced therapeutic performance can be attributed to the synergistic action between the biguanide and the bioactive lipophilic matrix. Sunflower and rosehip oils are exceptionally rich in polyunsaturated fatty acids, tocopherols, and

carotenoids, which are well-documented to promote tissue regeneration and modulate inflammatory responses [31,32]. Structurally, these components act down-stream to mitigate oxidative stress and regulate crucial cellular signaling pathways. This biochemical modulation is key to transitioning from the inflammatory to the proliferative phase of healing, ultimately leading to a down-regulation of pro-inflammatory cytokines, such as interleukin-1 (IL-1), interleukin-6 (IL-6), and tumor necrosis factor-alpha (TNF-α), and thereby establishing an optimized microenvironment for rapid re-epithelialization [33–35]. Literature evidence supports that rosehip oil promotes wound healing by accelerating the phenotypic transition of macrophages from the pro-inflammatory M1 phenotype to the M2 phenotype, which is associated with anti-inflammatory responses and tissue repair. This shift contributes to the resolution of inflammation and supports the regenerative phase of the healing process [36].

Additionally, the antimicrobial activity of PHMB contributes to the creation of a favorable microenvironment for tissue repair by reducing microbial load and associated inflammatory stimuli [11,28]. The nanometric droplet size of the formulation may further enhance this effect by improving the distribution and cellular interaction of the bioactive compounds, facilitating cell migration and accelerating wound closure as demonstrated in some studies [37–39]. Altogether, these findings suggest that the developed nanoemulsion promotes wound healing through a combination of antioxidant, anti-inflammatory, and antimicrobial mechanisms. The antimicrobial activity observed for the formulation can be attributed primarily to the PHMB presence, a cationic polymer widely recognized for its broad-spectrum antimicrobial properties. The mechanism of action of PHMB is mainly associated with electrostatic interactions between its positively charged biguanide groups and the

negatively charged components of bacterial cell membranes. This interaction disrupts membrane integrity, increasing permeability and ultimately leading to leakage of intracellular components and inhibition of microbial growth. In addition to membrane disruption, PHMB may also interact with intracellular targets such as bacterial DNA, further contributing to its antimicrobial efficacy [12,40].

PHMB-associated nanoemulsion system significantly enhances this antimicrobial efficacy by optimizing the dispersion of the active biguanide and maximizing its availability at the interface between the formulation and the microbial cells. The nanometric droplet size provides a vastly increased surface-to-volume ratio, which facilitates intimate contact between the cationic antimicrobial agent and the negatively charged bacterial membranes. This enhanced interfacial interaction disrupts membrane integrity more effectively, thereby increasing the overall efficiency of microbial inactivation. [14,28]. In addition, presence of vegetable oils in the formulation may provide complementary effects, as unsaturated fatty acids and minor bioactive constituents present in plant oils have been reported to exert mild antimicrobial activity. These lipophilic components directly interact with and destabilize microbial lipid membranes [41].

Another important aspect is the ability of such multifunctional formulations to simultaneously control microbial proliferation while maintaining a favourable environment for tissue repair [42]. By reducing the microbial burden, PHMB helps to prevent infection and limits the persistence of inflammatory stimuli associated with microbial colonization. This biological protection is highly critical in wound management, where bacterial contamination inevitably delays the healing cascade and exacerbates tissue damage. Therefore, the strategic integration of PHMB within an optimized nanoemulsion delivery system represents a highly promising and

synergistic approach for topical applications, successfully merging broad-spectrum antimicrobial defence with active support for tissue regeneration.

Conclusion

The results obtained in this study demonstrate that the developed nanoemulsion is a stable and scalable system with suitable physicochemical characteristics for topical applications. Experimental data corroborates with scalability of tested formulation even using a low energy method, a great evidence that composition and selected catastrophic emulsion phase inversion method is a viable approach for industrial production, despite minor variations associated with shear differences. These findings highlight the robustness of the system and its potential for large-scale manufacturing without compromising its nanotechnological properties.

From a biological perspective and therapeutic application, the PHMB-associated nanoemulsion exhibited multifunctional properties, combining antioxidant, antimicrobial, anti-inflammatory, and wound healing proprieties. The PHMB significantly enhanced antimicrobial efficacy and contributed to the modulation of inflammatory responses, while the vegetable oils in nanoemulsion seems contribute for reducing oxidative stress and promoting tissue regeneration.

Overall, these results indicate that the developed formulation represents a promising and scalable multifunctional platform for wound care applications, integrating antimicrobial protection with enhanced tissue repair capacity.

Experimental

Materials

PHMB chloride 20% aqueous solution was provided by IMCD Brasil (Diadema, SP, Brazil). Rosehip and sunflower oils were purchased from DPS química (Guarulhos, SP, Brazil). Polysorbate 80 was purchased from Sigma-Aldrich (Brazil). Sorbitan monooleate was purchased from Aquia Química (Guarulhos, SP, Brazil). Glycerol was purchased from Sciavicco (Belo Horizonte, MG, Brazil).

Production of nanoemulsions

ISnanoBio® PHMB nanoemulsion was initially produced in 10-gram batches using the phase inversion composition (PIC) method at room temperature (25 ± 2 °C). Briefly, the aqueous phase, composed by deionized water, poloxamer 407 (5%) and PHMB (1%), was added dropwise (1 mL/min) to the oil phase, composed by rosehip (1.4%) and sunflower (5.6%) oils, glycerol (10%), polysorbate 80 (5.25%) and sorbitan monooleate (1.75%) under 1500 rpm magnetic stirring (IKA® C MAG HS 7 magnetic stirrer).

Before to the addition of the aqueous phase, the oil phase was stirred for 5 minutes to achieve a sufficient homogenization of the ingredients. After this, the formulation was kept under stirring for 30 minutes. The entire process was conducted at room temperature (25 ± 2 °C). PHMB-free nanoemulsion (NE PHMB Free) was prepared in a similar manner, but in absence of PHMB. All samples were prepared in triplicate and data were expressed as mean ± standard deviation.

Scaling test

The 100 g and 1 kg batches were produced under mechanical stirring (IKA® RW 20 Digital mechanical stirrer) with an aqueous phase flow rate of 0.5 mL/min, and subsequently scaled up to 30 kg using a tilting process reactor (Alki Máquinas, Diadema, SP, Brazil) with an aqueous phase flow of 1 L/min. The conditions required to reach all scale-up stages are presented in Table 2. Furthermore, no changes to the composition were required to scale-up process.

Table 2 – Parameters for ISnanoBio® PHMB nanoemulsion production

Batch size	Equipment	Stirring speed (rpm)	Stirring duration (min)	Inclination angle	Temperature (°C)
10 g	IKA® C MAG HS 7 magnetic stirrer	1500	30	0	25
100 g	IKA® RW 20 Digital mechanical stirrer	1500	30	0	25
1 kg	IKA® RW 20 Digital mechanical stirrer	1600	30	0	25
30 kg	Tilting Process Reactor	3500	30	0	25

Physicochemical characterization

Diameter, Polydispersity Index (PdI) and Zeta Potential (ZP) were measured by dynamic light scattering (DLS) an equipment ZetaSizer NanoZS (Malvern Instruments, UK) with the aid of Zeta Plus® Particle Sizing software version 8.01, at a wavelength of 659 nm with a scattering angle of 173° and temperature at 25 °C with a 1:100 dilution.

Stability test

The preliminary stability of the formulation prepared using a mechanical propeller stirrer was evaluated for 15 days according to the *Cosmetic Products Stability Guide* issued by the Agência Nacional de Vigilância Sanitária (1st ed., Brasília: ANVISA, 2004, 52 p.). For room temperature the samples were evaluated for 180 days at predetermined intervals.

The evaluated parameters included appearance, color, and odor, which were assessed by visual inspection; pH, measured using a benchtop pH meter (Gehaka equipment) with a specific electrode; mean droplet diameter and polydispersity index, determined by dynamic light scattering; and zeta potential, measured by electrophoretic mobility using a Zetasizer Nano ZS (Malvern Panalytical).

The samples were stored in hermetically sealed, opaque containers protected from light. The storage conditions were as follows: room temperature (25 ± 2 °C); elevated temperature in an oven (40 ± 2 °C); low temperature under refrigeration (5 ± 2 °C); and freeze–thaw cycles, consisting of alternating storage for 24 h in a refrigerator (3 ± 2 °C) and 24 h in an oven (38 ± 2 °C) over a period of 15 days (except for room temperature samples, which were evaluated for 180 days).

Efficacy study

Antioxidant activity

Antioxidant capacity was measured by DPPH radical scavenging assay. Samples were added to a 0,1 mM DPPH solution and incubated at 25°C in dark for 60 minutes and a blank measure was made for every sample to avoid the light

scattering effect. After incubation, the absorbance was measured at 517 nm with an Agilent Epoch BioTek microplate reader.

Moisturizing effect

The moisturizing effect was evaluated using a transmembrane water loss (TMWL) assay as described previously by Montenegro and colleagues in 2017, with modifications [43]. Briefly, a cellulose membrane was placed over a beaker containing 10 mL of water. A thin layer of the formulation was then applied onto the membrane surface. The beaker was subsequently placed in an oven maintained at 32 ± 0.5 °C for 6 h.

The beakers were weighed at the beginning and at the end of the experiment, and the difference in mass was used to determine the amount of water lost by evaporation. All measurements were performed in triplicate. A control experiment was also conducted under the same conditions using a cellulose membrane without any formulation applied.

Anti-inflammatory activity

For anti-inflammatory evaluation, human keratinocyte cultures were maintained in DMEM (Dulbecco's Modified Eagle's Medium) supplemented with appropriate additives, incubated at 37 °C in a humidified atmosphere containing 5% CO_2, and handled under a laminar flow hood. The cells were seeded into culture plates and subjected to cellular stress induced by sodium lauryl sulfate (SLS). Subsequently, solutions corresponding to the control and sample groups were applied, and the cells were incubated for 48 h under the same conditions. After this

period, messenger RNA (mRNA) was extracted using Trizol reagent, and its quantity and purity were evaluated.

The extracted RNA was then subjected to reverse transcription to synthesize complementary DNA (cDNA). Gene expression analysis of IL-1, IL-6, and TNF-α was subsequently performed, using GAPDH as the endogenous control. The tested concentrations were 0.05% for ISnanoBio® PHMB, 0.001% for PHMB, and 1% for the Commercial PHMB Solution.

Wound healing

Human epidermal keratinocytes were used in this study. The cells were cultured in DMEM (Dulbecco's Modified Eagle's Medium) supplemented with appropriate additives, maintained at 37 °C in a humidified atmosphere containing 5% CO_2, and handled under a laminar flow hood. The cells were seeded into appropriate culture plates for cell growth. A preliminary cytotoxicity assay was conducted to determine non-cytotoxic concentrations for the efficacy analysis. The concentrations selected for the study were 0.05% ISnanoBio® PHMB, 0.001% PHMB, and 1.0% Market Product (0.1% PHMB in its composition).

For the control group, cells were maintained in supplemented culture medium. When the cultures reached 100% confluence, an in vitro wound was created, which was defined as time 0 h. At this point, supplemented culture medium was added to the control group, while the experimental groups received the test solutions. The cultures were then maintained at 37 °C for 48 h, and images were captured every 12 h for comparison.

The images were analyzed using the ImageJ software. The wound areas were measured at 0, 12, 24, 36, and 48 h to determine the percentage of wound closure over time. The wound area at 0 h was considered 0% closure, while 100% closure was defined as the point at which the bottom of the culture plate was no longer visible.

Antimicrobial effect

The antibacterial activity was evaluated using the broth microdilution method, following the methodology described by the Clinical and Laboratory Standards Institute (CLSI, 2012), with minor modifications. The bacterial strains were obtained from the Biotechnology of Biomolecules Laboratory of the Department of Biochemistry, Federal University of Rio Grande do Norte. The Gram-positive bacterium *Staphylococcus aureus* (ATCC 29213) and the Gram-negative bacterium *Escherichia coli* (ATCC 25922) were used. The strains were maintained on nutrient agar (HIMEDIA, India) at 4 °C.

The bacteria were streaked onto Mueller–Hinton agar (MH, HIMEDIA, India) and incubated for 24 h at 35 ± 2 °C. After incubation, a microbial suspension was prepared in sterile tubes containing 0.9% saline solution, and the turbidity was adjusted to the 0.5 McFarland standard at 595 nm using a microplate reader (Epoch-BioTek®, Winooski, VT, USA).

In 96-well microplates, mixtures containing different concentrations of the samples and the bacterial suspension in MH broth (5×10^5 CFU/mL) were incubated at 35 ± 2 °C for 24 h. Wells containing culture medium in the presence and absence of the bacterial suspension were used as positive and negative controls for microbial growth, respectively.

After the incubation period, the absorbance was measured at 595 nm using a microplate reader. The results were expressed as the percentage of microbial growth relative to the positive growth control. The minimum inhibitory concentration (MIC) was defined as the lowest sample concentration capable of inhibiting visible microbial growth, presenting absorbance values similar to those of wells containing culture medium in the absence of bacterial suspension.

Acknowledgements

The authors would like to thank the Laboratory of Pharmaceutical Technology and Biotechnology (TECBIOFAR) and the Distributed Systems Laboratory (LaSiD), both at the Department of Pharmacy, Federal University of Rio Grande do Norte, for providing the equipment and technical support required to perform the analyses. The authors also thank Professor Matheus Pedrosa, Ph.D., Coordinator of the Biotechnology Biomolecule Laboratory, Department of Biochemistry, Federal University of Rio Grande do Norte, for his valuable support and the antimicrobial evaluation.

Competing Interests

Mariana Silva and Daniele Gomes hold operational roles and are affiliated with ISnano®, a company that produces, markets, and sells nanoemulsions, such as the sunflower and rosehip oil nanoemulsion that is the subject of this article. Arnóbio A. da Silva-Júnior and Ednaldo G. do Nascimento are founding partners and hold equity interests in ISnano® without an employment contract with the company. The Federal University of Rio Grande do Norte (UFRN) is their primary institutional affiliation. Eron Lincoln Alves-Pereira, whose primary institutional affiliation is also UFRN,

collaborates as a Research and Development Analyst in joint projects between UFRN and ISnano®. This study was partially supported by ISnano®.

References

(1) Canchy, L.; Kerob, D.; Demessant, A.; Amici, J. M. Wound Healing and Microbiome, an Unexpected Relationship. *Journal of the European Academy of Dermatology and Venereology*. John Wiley and Sons Inc March 1, **2023**, pp 7–15. doi:10.1111/jdv.18854

(2) Klaas, M.; Mäemets-Allas, K.; Cárdenas-León, C. G.; Jaks, V. Cutaneous Wound Healing—Insights from the Matricellular Perspective. *FEBS Letters*. John Wiley and Sons Inc **2025**. doi:10.1002/1873-3468.70220

(3) Poljšak, N.; Glavač, N. K.; Ravnikar, M.; Jeras, M. *Sci. Rep.* **2025**, *15*. doi:10.1038/s41598-025-09711-7

(4) Lim, H. C.; Lee, S. K.; Keng, J. W.; Lee, E. Q.; Tan, E. S. S.; Liew, K. Bin; Mai, C. W.; Lee, S. K.; Chen, L.; Low, M. L.; Chew, Y. L. *Drug Deliv. Transl. Res.* **2025**, *15*, 4260–4276. doi:10.1007/s13346-025-01939-0

(5) Aydin Acar, C.; Kiyak, F. G.; Pehlivanoglu, S.; Yesilot, S.; Ozmen, O. *3 Biotech* **2025**, *15*. doi:10.1007/s13205-025-04498-w

(6) Dourado, D.; Rocha Formiga, F.; Do, É.; Alencar, N.; Reynaud, F. *Beilstein J. Nanotechnol* **2026**, *17*, 555–558. doi:10.3762/bjnano.17.36

(7) Erdoğar, N.; Gür, B.; Örgül, D. Recent Developments of Novel Nanotechnology-Based Drug Delivery Systems for Dermal and Transdermal Applications. *European Journal of Pharmaceutical Sciences*. Elsevier B.V. February 1, **2026**. doi:10.1016/j.ejps.2025.107413

(8) Rai, V. K.; Mishra, N.; Yadav, K. S.; Yadav, N. P. *Journal of Controlled Release* **2018**, *270*, 203–225. doi:10.1016/j.jconrel.2017.11.049

(9) Uberoi, A.; McCready-Vangi, A.; Grice, E. A. *Nature Reviews Microbiology 2024 22:8* **2024**, *22*, 507–521. doi:10.1038/s41579-024-01035-z

(10) Zielińska, M.; Pawłowska, A.; Orzeł, A.; Sulej, L.; Muzyka-Placzyńska, K.; Baran, A.; Filipecka-Tyczka, D.; Pawłowska, P.; Nowińska, A.; Bogusławska, J.; Scholz, A. *International Journal of Molecular Sciences 2023, Vol. 24, Page 17318* **2023**, *24*, 17318. doi:10.3390/IJMS242417318

(11) Teng, V. C.; Madjid, A.; Widita, W.; Djawad, K. The Efficacy and Safety of Polyhexanide Compared to Other Wound Dressings in Patients with Various Wound Types: A Systematic Review and Meta-Analysis. *Wound Practice and Research*. Cambridge Media September 1, **2025**, pp 122–138. doi:10.33235/wpr.33.3.122-138

(12) Rippon, M. G.; Rogers, A. A.; Ousey, K. *Polyhexamethylene Biguanide and Its Role in Wound Healing: A Narrative Review*; **2023**

(13) Abri, S.; Ghatpande, A. A.; Ress, J.; Barton, H. A.; Leipzig, N. D. *ACS Appl. Bio Mater.* **2019**, *2*, 5848–5858. doi:10.1021/acsabm.9b00833

(14) Ni, Y.; Qian, Z.; Yin, Y.; Yuan, W.; Wu, F.; Jin, T. *Molecules* **2020**, *25*. doi:10.3390/molecules25061334

(15) Prakash, V.; Parida, L. *Results in Engineering* **2023**, *18*. doi:10.1016/j.rineng.2023.101175

(16) Gorjian, H.; Mihankhah, P.; Khaligh, N. G. *J. Mol. Liq.* **2022**, *359*, 119379. doi:10.1016/j.molliq.2022.119379

(17) Fañani, A.; Arcos-Álvarez, B.; Banegas, P.; Rocha, L.; Monge-Corredor, J.; Rubio, R. G.; Guzmán, E.; Lucia, A. *Colloids Surf. A Physicochem. Eng. Asp.* **2025**, *704*. doi:10.1016/j.colsurfa.2024.135474

(18) Einstein, A. *Zur Elektrodynamik Bewegter Körper*; **1905**; Vol. 322. doi:10.1002/andp.19053221004

(19) Guo, Y.; Zhang, X.; Wang, X.; Zhang, L.; Xu, Z.; Sun, D. *Langmuir* **2024**, *40*, 1364–1372. doi:10.1021/acs.langmuir.3c03019

(20) Turan, S.; Solak, R.; Kiralan, M.; Ramadan, M. F. *Grasas y Aceites* **2018**, *69*. doi:10.3989/gya.1114172

(21) de Oliveira, J. B.; Michels, F. S.; Silva de Pádua Melo, E.; Nazário, C. E. D.; Caires, A. R. L.; Gonçalves, D. A.; Cardoso, C. A. L.; Aragão do Nascimento, V. *Data Brief* **2019**, *26*. doi:10.1016/j.dib.2019.104427

(22) Rajkumar, J.; Chandan, N.; Lio, P.; Shi, V. *Skin Pharmacol. Physiol.* **2023**, *36*, 174–185. doi:10.1159/000534136

(23) Kouhsoltani, M.; Hamishehkar, H.; Same, S.; Adibkia, K.; Zarza, K.; Shokri, J.; Taghaee, M.; Kouhsoltani, M. *A Comparative Histological Study on the Skin Occlusion Performance of a Cream Made of Solid Lipid Nanoparticles and Vaseline*; **2015**; Vol. 10

(24) Loo, C. H.; Basri, M.; Ismail, R.; Lau, H. L. N.; Tejo, B. A.; Kanthimathi, M. S.; Hassan, H. A.; Choo, Y. M. *Int. J. Nanomedicine* **2013**, *8*, 13–22. doi:10.2147/IJN.S35648

(25) Liakopoulou, A.; Letsiou, S.; Avgoustakis, K.; Hatziantoniou, S. *Cosmetics* **2025**, *12*. doi:10.3390/cosmetics12030102

(26) Ciarcià, G.; Bianchi, S.; Tomasello, B.; Acquaviva, R.; Malfa, G. A.; Naletova, I.; La Mantia, A.; Di Giacomo, C. *Biomedicines* **2022**, *10*. doi:10.3390/biomedicines10102473

(27) Coniglio, S.; Shumskaya, M.; Vassiliou, E. *Biology (Basel).* **2023**, *12*, 17

(28) Liu, D.; Yu, T.; Ma, S.; Su, L.; Zhong, S.; Wang, W.; Liu, Y.; Yu, J. A.; Gao, M.; Chen, Y.; Xu, H.; Liu, Y. *Journal of Nanobiotechnology* **2025**, *23*. doi:10.1186/s12951-025-03398-8

(29) Negrean, O. R.; Farcas, A. C.; Nemes, S. A.; Cic, D. E.; Socaci, S. A. Recent Advances and Insights into the Bioactive Properties and Applications of Rosa Canina L. and Its by-Products. *Heliyon*. Elsevier Ltd May 15, **2024**. doi:10.1016/j.heliyon.2024.e30816

(30) Lin, T. K.; Zhong, L.; Santiago, J. L. Anti-Inflammatory and Skin Barrier Repair Effects of Topical Application of Some Plant Oils. *International Journal of Molecular Sciences*. MDPI AG January 1, **2018**. doi:10.3390/ijms19010070

(31) Oargă, D. P.; Cornea-Cipcigan, M.; Cordea, M. I. Unveiling the Mechanisms for the Development of Rosehip-Based Dermatological Products: An Updated Review. *Frontiers in Pharmacology*. Frontiers Media SA **2024**. doi:10.3389/fphar.2024.1390419

(32) Pereira Oliveira, C. N.; Nani Leite, M.; de Paula, N. A.; Araújo Martins, Y.; Figueiredo, S. A.; Cipriani Frade, M. A.; Lopez, R. F. V. *Pharmaceutics* **2023**, *15*. doi:10.3390/pharmaceutics15030999

(33) Mazzocchi, A.; De Cosmi, V.; Risé, P.; Milani, G. P.; Turolo, S.; Syrén, M. L.; Sala, A.; Agostoni, C. Bioactive Compounds in Edible Oils and Their Role in Oxidative Stress and Inflammation. *Frontiers in Physiology*. Frontiers Media S.A. April 30, **2021**. doi:10.3389/fphys.2021.659551

(34) Poljšak, N.; Glavač, N. K.; Ravnikar, M.; Jeras, M. *Sci. Rep.* **2025**, *15*. doi:10.1038/s41598-025-09711-7

(35) Poljšak, N.; Kreft, S.; Kočevar Glavač, N. Vegetable Butters and Oils in Skin Wound Healing: Scientific Evidence for New Opportunities in Dermatology.

Phytotherapy Research. John Wiley and Sons Ltd February 1, 2020, pp 254–269. doi:10.1002/ptr.6524

(36) Lei, Z.; Cao, Z.; Yang, Z.; Ao, M.; Jin, W.; Yu, L. *Planta Med.* **2019**, *85*, 563–569. doi:10.1055/a-0725-8456

(37) Mohamed, N. K.; Metwally, A. A.; Fared, S. M. Y.; Farid, A.; Taha, M. *Colloids Surf. B Biointerfaces* **2025**, *245*. doi:10.1016/j.colsurfb.2024.114312

(38) Feng, C.; Xin, W.; Reyanggu, A.; Xueping, M.; Sodik, N.; Tao, W.; Bakri, M.; Maitinuer, M. *Ind. Crops Prod.* **2025**, *233*. doi:10.1016/j.indcrop.2025.121371

(39) Kaplan, A. B. U.; Yesilyurt, F.; Guven, L.; Cetin, M.; Lacin, B. B.; Ozkaraca, M.; Yilmaz, M. A.; Hacimuftuoglu, A.; Kaya, Y. *South African Journal of Botany* **2024**, *168*, 316–327. doi:10.1016/j.sajb.2024.03.026

(40) Sowlati-Hashjin, S.; Karttunen, M.; Carbone, P. *Journal of Physical Chemistry B* **2020**, *124*, 4487–4497. doi:10.1021/acs.jpcb.0c02609

(41) Pérez-López, M.; García-Contreras, R.; Soto-Hernández, M.; Rodríguez-Zavala, J. S.; Martínez-Vázquez, M.; Prado-Galbarro, F. J.; Castillo-Juárez, I. *J. Med. Food* **2018**, *21*, 356–363. doi:10.1089/jmf.2017.0080

(42) Hu, Y.; Yu, L.; Dai, Q.; Hu, X.; Shen, Y.; Shen, Y. *Biomater. Sci.* **2024**, *12*, 2460–2479. doi:10.1039/d4bm00155a

(43) Montenegro, L.; Parenti, C.; Turnaturi, R.; Pasquinucci, L. *Pharmaceutics* **2017**, *9*. doi:10.3390/pharmaceutics9040058